BREAKER BAR FORMATION AND MIGRATION

Bart T. Grasmeijer[1] and Leo C. van Rijn[1, 2]

Abstract

The formulation of Isobe and Horikawa (1982) is modified and adapted for use in a probabilistic cross-shore transport model (CROSMOR). Computed changes of wave height, peak near-bed orbital velocity and depth-averaged return flow are compared to laboratory measurements. A comparison is made between computed and measured bed profile changes for a large scale laboratory experiment.

Introduction

The generation and maintenance of longshore bars is commonly associated with the shoaling and breaking of high-frequency waves and the generation of low-frequency wave effects in the surf zone. Breaker bars may be generated and maintained by a combination of spilling and shoaling waves; the latter producing landward sediment transport due to wave asymmetry and increasing toward the break point, thereafter reducing and grading into seaward transport by undertow currents associated with spilling breakers leading to build up of the bar. Although formation and maintenance of bars may also be related to low-frequency waves, in this paper attention will be focused on the convergent pattern of sediment fluxes due to wave asymmetry and undertow. Model calculations are compared to a small and a large scale laboratory tests.

Model description

The cross-shore transport model is based on a wave by wave approach (Wijnberg and Van Rijn, 1996). The probability density function of the deep water wave height is schematised into a discrete series of wave height classes and corresponding periods. Each wave height class is assumed to propagate independently of the other classes by solving the wave energy balance separately. The waves shoal until an empirical criterion for breaking is satisfied. Wave height decay after breaking is modelled by dissipation of energy in a breaking wave and a bore. Tide, wave, and storm induced water level variations and tide, wind and wave driven longshore currents are also included in the model.

The high-frequency near-bed orbital velocities (low-frequency effects are neglected) are computed using a modification of the method of Isobe and Horikawa (1982). The method of Isobe and Horikawa method is a parameterisation of fifth-order Stokes wave theory and third-order cnoidal wave theory which can be used over a wide range

[1] Dep. of Phys. Geography, Univ. of Utrecht, P.O. Box 80.115, 3508 TC, Utrecht, The Netherlands, e-mail: B.Grasmeijer@geog.uu.nl

[2] Delft Hydraulics, P.O.Box 177, 2600 MH, Delft, The Netherlands, e-mail: Leo.vanRijn@wldelft.nl

of wave conditions. In the original formulation the near-bed value of û (defined as: u_{on} + u_{off}) is derived from deep water wave conditions as follows:

$$\hat{u} = 2.r.u_{linear} \tag{1}$$

with:

$$r_3 = -27.3 \log_{10}\left(\frac{H_0}{L_0}\right) - 16.3 \tag{2}$$

$$r_2 = 1.28 \tag{3}$$

$$r_1 = 1 \tag{4}$$

$$r = r_1 - r_2 \exp\left\{-r_3 \frac{h}{L_0}\right\} \tag{5}$$

u_{linear} = peak near-bed velocity computed using linear wave theory (m/s), H_0 = deep water wave height (m), L_0 = deep water wave length (m), h = local water depth (m).

Hamm (1996) tested the formulation from Isobe and Horikawa and the formulation from Swart and Crowley (1988) against laboratory measurements. He found that the Isobe and Horikawa formulation can be used over a large range of wave conditions except in the surf zone when monochromatic waves are considered. Although the covocoïdal theory from Swart and Crowley provides a more comprehensive description of wave properties, abnormal results were observed in a few cases. The use of one representative wave height and period in random waves may lead to an underestimation of velocity moments with low steepness waves.

Stripling and Damgaard (1997) adapted the method from Isobe and Horikawa for use in a model for morphodynamic predictions. They compared the results with vocoidal theory (Swart, 1978). Although vocoidal theory consistently over-predicted the values of the odd bottom velocity moments and the method of Isobe and Horikawa consistently under-predicted them by a similar order, the most important aspect of their comparison was not so much in the values of the moments but rather the direction in which the methods predict the moments to be in. Vocoidal theory occasionally predicted the odd moments in the opposite direction to the measurements, which was not so with the method of Isobe and Horikawa (1982). Compared to vocoidal theory the method of Isobe and Horikawa led to greater accuracy in the morphodynamic prediction capability of the profile model.

In the present modified formulation the near-bed value of û is derived from the local wave conditions as follows:

$$r = 1 - 3.2\left(\frac{H}{L}\right)^{065}\left(\frac{H}{L}\right)^{3.4\frac{h}{L}} \tag{6}$$

with: H = local wave height (m), L = local wave length (m), u_{linear} = near-bed velocity computed using linear waves theory.

The r factor was found by calibration using laboratory and field data with random waves. Basic data are given in Table 1.

Description	Testnumber	h (m)	H_{m0} (m)	T_p (s)
Field: Terschelling, The Netherlands	Fop05330	9.0	1.89	8.0
	Fop17352	9.4	0.37	17.1
	Fop17576	10.5	4.20	10.2
	Fra05330	5.6	1.87	8.0
	Fra17576	7.7	3.42	9.7
	Fre05330	4.1	1.70	8.1
	Fre17352	5.4	0.37	16.5
Field: Egmond aan Zee, The Netherlands	1B_04430	1.9	0.76	6.1
Lab: small scale flume Delft Univ. of Techn.	TUDB2_01	0.60	0.18	2.2
	TUDB2_05	0.31	0.17	2.2
	TUDB2_07	0.51	0.15	2.2
Field: Muriwai, New Zealand	Muriwai2	1.83	0.92	19.7
Field: Skallingen, Denmark	Sk304_08	1.8	0.80	11.0
	Sk310_01	2.6	1.49	8.8
Lab: Delta Flume Lip11D WL Delft Hydraulics	1A0203_02	2.31	0.92	5.0
	1A0203_07	0.91	0.62	5.0
	1B0213_02	2.30	1.19	5.0
	1B0213_07	0.89	0.57	5.0
	1C0204_02	2.25	0.63	8.0
	1C0204_03	1.77	0.63	8.0
	1C0204_05	1.16	0.63	8.0
	1C0204_11	1.59	0.63	8.0

Table 1. Basic data of measurements used in calibration of r factor.

Measured signals of surface elevation and horizontal orbital velocity near the bed were analysed using spectral analysis. High- and low-frequency oscillations were separated (by filtering) at a period of 2 times the wave spectrum peak period, T_p. The high-frequency signals were separated into shorter time series each containing 10-15 individual waves. Each of the short time series was defined as one single wave class with one representative wave height, wave period, crest velocity near the bed, and trough velocity near the bed. The mean values were chosen to represent the wave class. A comparison between measured and computed values of $\hat{u}$ is presented in Figure 2. The broken lines indicate a 20% error band.

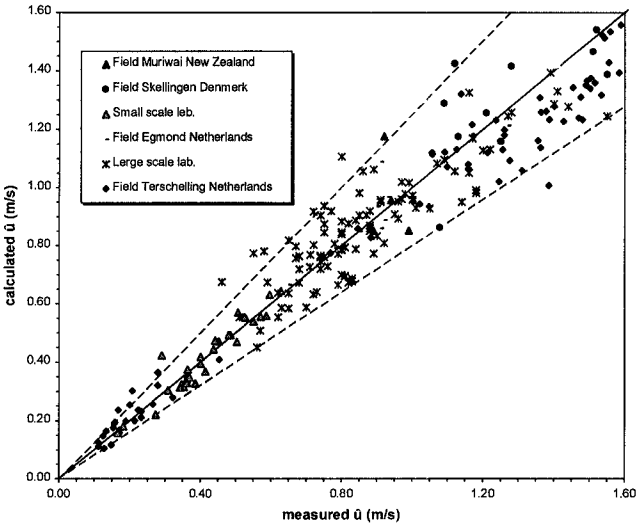

Figure 1. Comparison between measured and computed values of near-bed orbital velocity û defined as $u_{on} + u_{off}$.

The following formulae, Eq.(7)-Eq.(14), were derived to account for the asymmetry of the velocity profile (Isobe and Horikawa, 1982). Eq.(7)-Eq.(12) is a parameterisation of fifth-order Stokes wave theory and third-order cnoidal wave theory. Eq.(13) and Eq.(14) were introduced to take into account the deformation of the velocity profile due to bottom slope.

$$\left(\frac{u_{on}}{\hat{u}}\right)_a = \lambda_1 + \lambda_2\left(\frac{\hat{u}}{\sqrt{gh}}\right) + \lambda_3 \exp\left(-\lambda_4\left(\frac{\hat{u}}{\sqrt{gh}}\right)\right) \tag{7}$$

with:

$$\lambda_1 = 0.5 - \lambda_3 \tag{8}$$

$$\lambda_2 = \lambda_3\lambda_4 + \lambda_5 \tag{9}$$

$$\lambda_3 = \frac{(0.5 - \lambda_5)}{\lambda_4 - 1 + \exp(-\lambda_4)} \tag{10}$$

$$\lambda_4 = \begin{cases} -15 + 1.35\left(T\sqrt{\frac{g}{h}}\right), & T\sqrt{\frac{g}{h}} \le 15 \\ -2.7 + 0.53\left(T\sqrt{\frac{g}{h}}\right), & T\sqrt{\frac{g}{h}} > 15 \end{cases} \tag{11}$$

$$\lambda_5 = \begin{cases} 0.0032\left(T\sqrt{\frac{g}{h}}\right)^2 + 0.000080\left(T\sqrt{\frac{g}{h}}\right)^3, & T\sqrt{\frac{g}{h}} \le 30 \\ 0.0056\left(T\sqrt{\frac{g}{h}}\right)^2 - 0.000040\left(T\sqrt{\frac{g}{h}}\right)^3, & T\sqrt{\frac{g}{h}} > 30 \end{cases} \quad (12)$$

$$\left(\frac{u_{on}}{\hat{u}}\right)_{modified} = 0.5 + \left(\left(\frac{u_{on}}{\hat{u}}\right)_{max} - 0.5\right)\tanh\left(\frac{\left(\frac{u_{on}}{\hat{u}}\right)_a - 0.5}{\left(\frac{u_{on}}{\hat{u}}\right)_{max} - 0.5}\right) \quad (13)$$

with:

$$\left(\frac{u_{on}}{\hat{u}}\right)_{max} = 0.62 + \frac{0.003}{\text{bed slope}} \quad (14)$$

A comparison between preliminary computations using the present probabilistic model and laboratory tests showed that the influence of the bed slope might be less pronounced. The following relation gave more realistic results:

$$\left(\frac{u_{on}}{\hat{u}}\right)_{max} = 0.62 + \frac{0.001}{\text{bed slope}} \quad (15)$$

The present model includes a sinusoidal distribution of the instantaneous velocities during the forward and backward phase of the wave cycle. The duration period of each phase is corrected to obtain zero net flow over the full cycle. This is in contrast to the original approach of Isobe and Horikawa.

The depth-averaged return current under the wave trough of each individual wave (summation over wave classes) is approximated with the following expression:

$$U_{mean,return} = 0.125\sqrt{\frac{g}{h}}\frac{H_{rms}^2}{h_t} \quad (16)$$

in which H_{rms} = root-mean-square wave height, h = mean water depth, averaged over half a wave length seawards, h_t = water depth below wave trough level defined as h-½H_{rms}. Equation (16) is based on linear mass flux ($q = U_{mean}\, h_t = 0.125\, g\, H^2/c$), an effective depth equal to h_t (=depth below wave trough) and $c=(gh)^{0.5}$ = wave propagation speed in shallow water.

The sand transport rate of the model is determined for each wave (or wave class), based on the computed wave height, depth-averaged cross-shore and longshore velocities, orbital velocities, friction factors and sediment parameters. Net transport rates are obtained after time-averaging of instantaneous values over the wave period. The sediment transport model is local and horizontal advection of sediment clouds due to mean currents and long period oscillations is not considered. The net (averaged over the wave period) total sediment transport is obtained as the sum of the net bed load (q_b) and net suspended load (q_s) transport rates.

Small Scale Laboratory Test

The cross-shore transport model was used to compute the hydrodynamics measured during a small scale laboratory test. The tests were conducted in the Large Research

Flume of the Laboratory of Fluid Mechanics of the Faculty of Civil Engineering (Delft University of Technology).

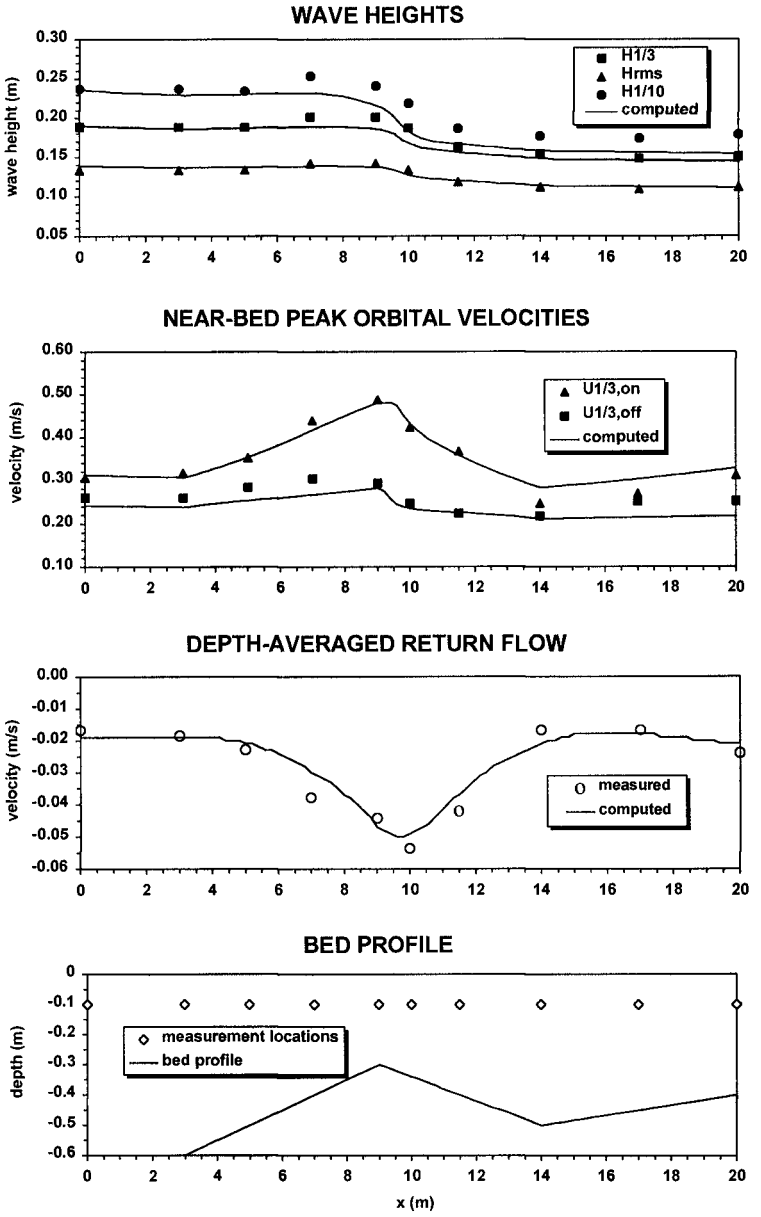

Figure 2. Measured and computed wave heights, peak orbital velocities and depth-averaged return flows for small scale laboratory test.

The flume has a length of 45 m, a width of 0.8 m and a depth of 1.0 m. Irregular waves (following a Jonswap spectrum) were generated with a peak spectral period of, T_p = 2.3 s (± 0.2 s). A nearshore bar of the form shown in Figure 2 was generated in the flume. The bed profile varies in depth from 0.60 m seawards of the bar to 0.30 m at the bar crest (Figure 2). The water depth in the trough landward of the bar crest is 0.50 m. The nearshore bar has a steep seaward slope of 1 to 20 and a steep landward slope of 1 to 25. The bed slope landward of the bar trough is 1 to 63. Measurements were performed at 10 different locations across the nearshore bar. Herein the test with an initial wave height of 0.19 m (B2) is considered. Figure 2 shows the measured and computed wave heights, peak orbital velocities and depth-averaged return flows. It can be observed that in the region near the bar crest the computed $H_{1/3}$ and $H_{1/10}$ values are about 10% too small, which may be caused by the use of linear wave theory. Better agreement between measured and computed wave heights may be obtained by using non-linear shoaling. The computed and measured return flow values show reasonably good agreement. From Figure 2 it can be observed that the significant values of the near-bed peak orbital velocities can be predicted with reasonable accuracy using the modified Isobe and Horikawa formulation. The depth-averaged return flow is rather accurately predicted by the model.

Large Scale Laboratory Tests

The model has been applied to compute the hydrodynamics and morphodynamics measured during large scale laboratory tests (Roelvink and Reniers, 1995). The tests were conducted in the Delta Flume of Delft Hydraulics. The Delta Flume is a large flume with the following dimensions: length = 200 m, width = 5 m and depth = 7 m. Three different test conditions were simulated: slightly erosive wave conditions, highly erosive wave conditions and strongly accretive wave conditions. The bed consisted of fine to medium coarse sand (D_{50} = 200 μm and D_{90} = 400 μm). Before and after each test the bed levels were measured in three longitudinal sections. Irregular waves (following a Jonswap spectrum) were generated. The wave board driving system was compensated for the reflection of long waves in the flume. Water level variations were measured by pressure sensors and by resistance type wave gauge at various locations in the flume. Herein, the test with highly erosive wave conditions (test 1b) is considered. The incident wave conditions are: H_{m0} = 1.40 m, T_p = 5.0 s, duration = 6 hours. Figure 3 shows the computed and measured wave heights, peak orbital velocities and depth-averaged return flows. The computed wave heights show fairly good agreement with the measurements with exception of an overestimation of H_{rms} in the region near the bar crest. It can be observed from Figure 3 that in the region seaward of the bar the significant values of the near-bed peak orbital velocities ($U_{1/3,on}$ and $U_{1/3,off}$) are reasonably well represented by the modified formulation of Isobe and Horikawa. Near the bar crest the onshore directed velocity is overestimated by the model while landward of the bar the offshore directed near-bed orbital velocity is slightly underestimated. The computed depth-averaged return flow shows good agreement with the measured values, except in the shallow surf zone (x > 160 m) where the depth-averaged return flow is significantly overestimated.

The initial bed profile and the measured and computed bed profiles after 6 hours of wave action are given in Figure 4. The measured profile shows an offshore migration of the bar, with erosion between 140 m and 160 m and accretion between 125 m and 140 m. The predicted profile also shows an offshore migration of the bar, however, this is too far seaward, with erosion between 138 m and 150 m and accretion between 110 m and 138 m.

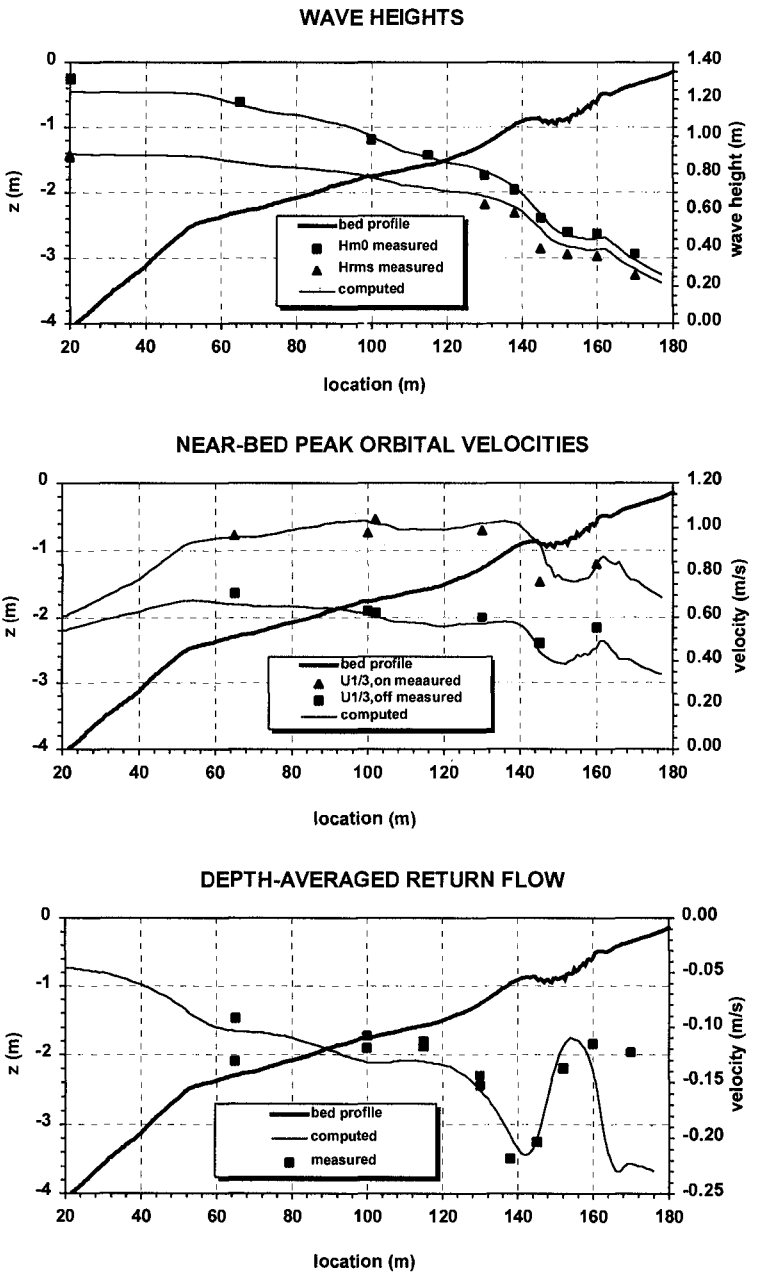

Figure 3. Measured and computed wave heights, peak orbital velocities and depth-averaged return flows for large-scale laboratory test.

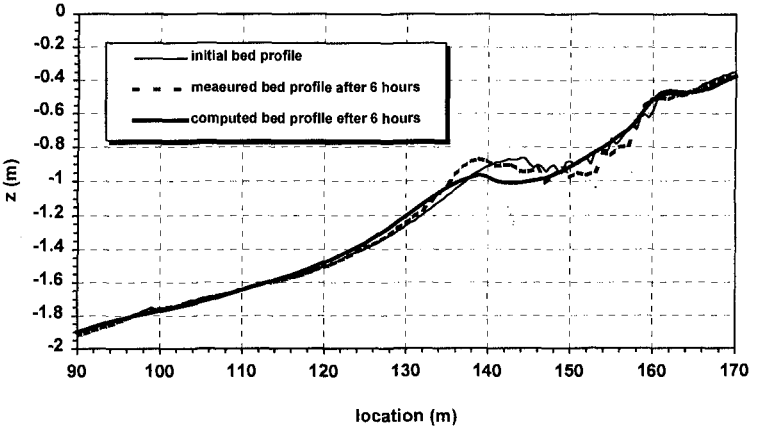

Figure 4. Measured and predicted bed profile change.

Conclusions

The formulation of Isobe and Horikawa (1982) was modified and adapted for use in a probabilistic cross-shore transport model. Comparison of model calculations and laboratory measurement showed that the near-bed orbital velocities could be predicted with reasonable accuracy using the method of Isobe and Horikawa (1982). However, the asymmetry of the orbital velocity was overestimated landward of the breakpoint. The depth-averaged mean return flow could reasonably well be represented using a simple formulation based on linear mass transport, except in the shallow surf zone where the depth-averaged mean return flow was significantly overestimated by the model. Further work is required to improve the morphodynamic predictions of the probabilistic cross-shore transport model.

References

Hamm, L., 1996. *Computation of near-bottom kinematics of shoaling waves, Proc. Int. Conf. on Coastal Engineering 1996, pp. 537-550.*

Isobe, M. and Horikawa, K., 1982. *Study on water particle velocities of shoaling and breaking waves, Coastal Engineering in Japan, Vol.25, 1982.*

Roelvink, J.A. and Reniers, A.J.H.M., 1995. *Lip11D Delta Flume Experiments, a profile dataset for profile model validation. Report H2130, January 1995, Delft Hydraulics, The Netherlands.*

Stripling, S. and Damgaard, J.S., 1997. *Improvement of morphodymamic predictions in COSMOS-2D, Report IT 443, March 1997, HR Wallingford, England.*

Swart, D.H., 1978. *Vocoidal water wave theory, Volume 1: Derivation, Nat. Res. Inst. for Oceanology, CSIR Report 357, Stellenbosch.*

Swart, D.H. and Crowley, J.B., 1988. *Generalised wave theory for a sloping bed, Proc. Int. Conf. on Coastal Engineering 1988, pp.181-203.*

Van Rijn, L.C. and Wijnberg, K.M., 1996. *One-dimensional modelling of individual waves and wave-induced longshore currents in the surf zone. Coast Engineering, Vol. 28, p.121-145*